International Journal of Applied Pharmaceutics

ISSN- 0975-7058 Vol 15, Issue 1, 2023

Original Article

INTRANASAL FORMULATION AND CHARACTERIZATION OF CHITOSAN MICROSPHERE FOR IMPROVING *IN VITRO* MUCOADHESION, RESIDENCE TIME AND ABSORPTION RATE OF PREGABALIN

ANIL PETHE, ANKITA HADKE, SURENDRA AGRAWAL, DARSHAN TELANGE*

Datta Meghe College of Pharmacy, Datta Meghe Institute of Higher Education and Research (Deemed to be University), Sawangi (Meghe), Wardha, Maharashtra, India 442001

***Email: darshan.pharmacy@dmimsu.edu.in**

Received: 15 Sep 2022, Revised and Accepted: 19 Oct 2022

ABSTRACT

Objective: Chitosan-based pregabalin microsphere (CBPM) formulation was prepared to improve *in vitro* mucoadhesion and absorption of pregabalin *via* intranasal administration.

Methods: The CBPM formulations were prepared using the inotropic gelation method and optimized using the Box-behnken design. The optimized CBPM formulation was physico-chemically characterized using scanning electron microscopy, thermal analysis, Fourier transform infrared spectrometry and powder x-ray diffraction. Additionally, the CBPM formulation was characterized for functional parameters such as *in vitro* mucoadhesion, *in vitro* drug release, *ex vivo* permeability across the sheep nasal mucosa and *in vivo* anticonvulsant activity in pentylenetetrazol (PTZ)-induced seizures model in mice.

Results: The design-optimized CBPM exhibited a 91.45 % inclusion efficiency of pregabalin in the microspheres. The Physico-chemical analysis of the individual components and the optimized formulation confirmed the formation of CBPM. The *in vitro* mucoadhesion study revealed ~80% mucoadhesive of the CBPM to the sheep nasal mucosa. The *in vitro* dissolution profiles of CBPM was significantly higher (~97%) than that of pure pregabalin (~70%). The CBPM displayed a higher rate and extent of permeability (~90%) than pure pregabalin (~76%) across the sheep nasal mucosa. The *in vivo* anticonvulsant activity showed that intranasal administration of CBPM resulted in significant ($P<0.01$) protection against PTZ-induced convulsions in mice.

Conclusion: The chitosan-based microsphere intranasal formulation could be employed as promising delivery for rapid pregabalin absorption.

Keywords: Chitosan microsphere, Pregabalin, Intranasal, Mucoadhesion, Anticonvulsant

DOI: https://dx.doi.org/10.22159/ijap.2023v15i1.46359. Journal homepage: https://innovareacademics.in/journals/index.php/ijap

INTRODUCTION

Pregabalin (PGB) is a first-line antiepileptic and analgesic drug used to treat diabetic neuropathy, partial neuropathy, and postherpetic neuralgia [1]. Commercially, it is available as a conventional capsule (Lyrica®) with a recommended dose of 75 mg twice a day and 50 mg three times a day to manage neuropathic pain and associated disorders [2]. PGB is an amino acid with desirable aqueous solubility [3]. Moreover, due to its low affinity for plasma proteins and a lack of hepatic metabolism, PGB demonstrates high oral absorption [4–6]. It is thus appropriately classified as a BCS class I drug. Despite PGB being a BCS class I drug with good solubility and permeability profile; however, the medical and clinical application of this molecule is limited by its unsuitable and unwanted biopharmaceutical properties, such as exhibiting multiple variations in absorption in the upper gastrointestinal tracts and requires frequent dosing of such a higher dose for maintaining therapeutic higher effects which ultimately resulted in causing dose-limiting side effects namely dizziness, sleepiness, dry mouth, blurred vision, difficulty with concentration, hyper-sensitivity and decreased platelet count once administrated orally [7, 8].

In recent times, several drug delivery systems have been investigated/explored for improving the delivery of PGB, including pulsatile delivery systems, nanoparticle systems, modified-release oral dosage forms, floating dosage forms and transdermal delivery systems, etc. [1, 2, 8, 9]. However, critical review and understanding of these systems demonstrated a minimal and minor improvement in the biopharmaceutical properties of PGB. Consequently, considering the limitations offered by the existing formulation system, we require a strong and potential alternative dosage form and delivery system that could be suitable for improving the delivery, reducing dosing frequency, and side effects of PGB.

Among all nanocarriers, the chitosan-based microsphere nanocarriers demonstrated the most recognizable formulation in improving the prolonged residence time of drugs, uniform absorption, controlled release of the drug, and drug loading capacity mucoadhesive of drugs. According to this, many scientists have employed this unique formulation strategy for improving the parameters mentioned above of several APIs and bioactive such as diclofenac sodium [10], clozapine [11], loratadine [12], tramadol hydrochloride [13]. Chitosan is a polycationic copolymer obtained from chitin via a deacetylation reaction. It holds one amino ($-NH_2$) and two hydroxyl {2(OH)} groups in the glucosidic residual chain. It is biocompatible and shows non-toxicity with living tissues. Moreover, it has a gel-forming capacity, high adsorption capacity, and biodegradable properties. These properties of chitosan make it a potential carrier for improving drug encapsulation efficiency and controlled release properties [14]. The mucoadhesive nature of chitosan (due to the cationic amino group) towards sialic and sulfonic acids (anionic group) in the mucosal layer exhibits electrostatic interactions. It further increases the drug's residence time and nasal epithelial permeability by opening the tight junction between the cells and reducing nasal clearance, resulting in improved drug biopharmaceutical performance. Chitosan formulations also provide multiple benefits: simple, reproducible, and efficient preparation methods, high loading capacity, and stability for a prolonged period. Earlier literature has shown that chitosan microspheres prepared using glutaraldehyde (as cross-linking agent) via the ionic gelation method significantly improved the biopharmaceutical properties of drugs [15–17]. Nasal drug delivery systems are considered to be one of the most attractive systems for rapid absorption of drugs like PGB, among other routes, due to the large absorption surface, a vascularized layer of epithelium, porous nature of the endothelial membrane, high blood flow, easy access, and importantly, lack of first-pass metabolism [18–20].

We prepared chitosan-based PGB microspheres (CBPM) using the current study simple and reproducible inotropic-gelation method. The formulation and process variables were optimized using the Box-behnken design. The optimized formulation was physico-chemically characterized by particle size analysis, zeta potential, thermal analysis, Fourier transform infrared spectroscopy and powder x-ray diffraction. The functional characterization of the formulation was carried out by *in vitro* mucoadhesion, *in vitro* diffusion, and *in vitro* permeation studies. Finally, the formulation's preliminary pharmacological and toxicological evaluation was carried out with histopathological and *in vivo* anticonvulsant activity studies.

MATERIALS AND METHODS

Pregabalin was obtained from Alkem Laboratories Ltd., Mumbai, India. Chitosan was obtained from HiMedia Laboratories Pvt. Ltd., Mumbai, India. Glutaraldehyde was obtained from Avantor Performance Materials India Ltd., Mumbai, India. Acetic acid, disodium hydrogen phosphate, and calcium chloride were obtained from Loba Chemicals Pvt. Ltd., Mumbai, India. Potassium chloride, potassium dihydrogen phosphate, and sodium chloride were obtained from Sigma Chemicals, Sigma-Aldrich Corporation, St. Louis, MO. All other chemicals used in the study were of analytical grade.

Preparation of pregabalin chitosan microspheres

Chitosan-based microspheres of pregabalin (CBPM) were prepared by the *ionotropic gelation method* reported earlier [21]. Briefly, accurately weighed chitosan (100, 150, or 200 mg) was dispersed into acetic acid (1% v/v, 30 ml). Pure pregabalin (PGB) was added to this dispersion and stirred to form a uniform mixture. Microspheres were formed by adding a cross-linking agent, glutaraldehyde (1, 1.5, or 2 ml), to the mixture at the rate of 30 drops/min *via* a disposable syringe (needle size 21G) and stirring the dispersion using a magnetic stirrer (800, 1000, or1200 RPM). The obtained microspheres were filtered, rinsed with deionized water, and dried in a hot air oven at 60 °C for 3 h. The moisture-free microspheres were then placed in light-protected glass vials, flushed with nitrogen, and stored at room temperature (25 °C) until further characterization.

Box-behnken design

In the present study, Box-Behnken design was employed using Design-Expert® (Version 10.0.4.0, Stat-Ease Inc., Minneapolis, Minnesota, USA) to understand the influence of selected formulation and process variables on the efficiency of pregabalin inclusion in the prepared microspheres. The independent variables for the study included the amount of chitosan (X_1, mg), stirring speed (X_2, RPM), and the amount of cross-linking agent (X_3, ml). Each of these variables was studied at three levels, *viz*. low (-1), medium (0), and high (+1), with the levels, were chosen based on previously published reports. The extent of pregabalin inclusion in the obtained microspheres (inclusion efficiency, % w/w) was used as a dependent variable. The design revealed 17 different combinations of variables for experimental trials. Thus, 17 trial formulations were prepared and evaluated for pregabalin inclusion. The results were then fitted to create a statistical model that took the shape of a polynomial equation (below). Various equation parameters, such as coefficient of magnitude and interaction terms were used to analyze and interpret the results.

$$Y=b0+b_1X_1+b_2X_2+b_3X_3+b_{11}X_1^2+b_{22}X_2^2+b_{33}X_3^2+b_{12}X_1X_2+b_{13}X_1X_3+b_{23}X_2X_3$$

Where Y is the entrapment efficiency (%, w/w), b_0 is the coefficient of the independent variable of X. The X_1, X_2, and $X_3$are the main effects exhibited at three levels. X_1X_2, X_1X_3, and X_2X_3 indicate the combined effects of independent variables. X_1^2, X_2^2, and X_3^2 represent the nonlinearity of the response. (table 1) shows the experimental design and actual values of the studied variables (table 2) shows the experimentally achieved PGB.

Table 1: Coded levels and "real" values for each factor studied

Variables	Levels		
	-1	0	+1
Independent	Real values		
Chitosan (X_1, mg)	100	150	200
Stirring speed (X_2, rpm)	800	1000	1200
Crosslinking agent (X_3, ml)	1.0	1.5	2.0
Dependent			
Inclusion efficiency (Y, % w/w)			

Inclusion efficiency (%)

The PGB inclusion efficiency in the prepared CBPM formulations was determined using a method previously described by Jeffery *et al.*[22]. Briefly, a carefully weighed amount of CBPM (containing ~10 mg PGB) was dispersed in phosphate buffer (10 ml, pH 6.6). The microspheres (CBPM) and any new chitosan theoretically dissolve in the buffer, whereas the non-encapsulated (free) PGB remains insoluble and forms a precipitate. The dispersion was centrifuged (Model: RM-12C, Remi Group, Mumbai, India) for 10 min at 560×g. After centrifugation, the supernatant was filtered (Whatman quantitative filter paper, ashless, grade 41, Sigma-Aldrich Corporation, St. Louis, MO). After appropriate dilutions, the absorbance of the resultant solution was analyzed spectroscopically (Model: SPECTRO UV 2060 Plus, Analytical Technologies Ltd. Gujarat, India) at 403 nm.

Particle size and zeta potential

The particle size distribution and the zeta potential measurements of the optimized CBPM formulation were carried out using Photon Cross-Correlation Spectroscopy (PCCS) with dynamic light scattering (DLS) technology. The study was followed as per method described earlier [23]. For particle size analysis, a carefully weighed amount (~5 mg) of CBPM was dispersed in 10 ml of deionized water, and the dispersion was analyzed (Model: NANOPHOX, Sympatec GmbH, Clausthal-Zellerfeld, Germany). All the experiment was carried out at room temperature (25 °C). The zeta potential of the optimized CBPM formulation was measured on a Nanoparticle Analyzer (Model: NanoPlusTM-2, Particulate Systems, Norcross, GA, USA) in the range of–200 to+200 mV.

Scanning electron microscopy

The surface morphology of the design-optimized CBPM formulation was characterized using a scanning electron microscope (Model: JSM 6390, JEOL Datum Ltd., Tokyo, Japan) with a resolution of 3.0 nm and a customizable Graphical User Interface (GUI). Briefly, the microsphere particles were carefully dusted on an aluminium stub, sputter-coated with gold to a thickness of ~400 A°, and scanned at different magnifications. Representative sample scans were analyzed and captured using the accompanying software (Smile Shot™). The earlier reported procedure has been employed for SEM analysis [24].

Thermal analysis

The thermograms of pure PGB, pure chitosan, the physical mixture (PM, 1:1.5) of PGB and chitosan, and the prepared CBPM were obtained on a differential scanning calorimeter (Model: DSC-1 821e, Mettler Toledo AG, Greifensee, Switzerland). The instrument was calibrated with indium standard and continuously purged with

nitrogen gas during operation. Accurately weighed samples (2.0±0.2 mg) were subjected to a single heating ramp cycle in a range of 40 °C to 400 °C at the rate of 10 °C/min. The obtained sample thermograms were analyzed using the software (Universal Analysis 2000, V4.5A, build 4.5.0.5) associated with the instrument. The already established method has been used for the thermal analysis of the samples mentioned above [25].

Fourier transform infrared spectroscopy

The molecular interactions between PGB and chitosan were studied by analyzing the FTIR spectra of pure PGB, pure chitosan, PM, and the prepared CBPM as per the earlier reported method [26]. Briefly, accurately weighed (~2 mg), moisture-free (dried) samples were weighed individually and triturated with potassium bromide (KBr, FT-IR grade, ~200 mg) to form a homogenous mixture. This mixture was then compressed into thin transparent discs using a Mini Hand Press (Model: MHP-1, P/N–200-66747-91, Shimadzu, Kyoto, Japan) at 10 tons/Nm2. This disc was used to obtain sample spectra on an FTIR spectrophotometer (Model: FTIR-8300, Shimadzu, Kyoto, Japan). Individual sample spectrum was acquired in a range of 4000 to 400 cm-1. The spectra were analyzed using the software (resolution FTIR control software, version 1.10) associated with the instrument.

Powder x-ray diffractometry

A powder x-ray diffractometer (Model: D8 ADVANCE, Bruker AXS, Inc., Madison, WI, USA) was used to analyze the crystalline behaviour of pure PGB, pure chitosan, PM, and CBPM. The analysis of these samples was carried out using earlier reported procedure [27]. Briefly, accurately weighed samples (~1g) were mounted onto the sample holder. The samples were then irradiated at a wavelength of (λ = 1.5406 A°) by a Cuκβ-based x-ray monochromatic radiation source. The operating voltage and current of the instrument were maintained at 40 mV and 35 mA, respectively. A one-dimensional detector (LINXEYE™) based on Bruker AXS compound silicon strip technology converted individual signals into a spectrum and monitored the sample diffraction patterns. The diffractograms of samples were obtained at a step angle of 0.02° on 2θ with the diffraction angle increasing from 30° to 60° and a step time of 29.1s.

***In vitro* mucoadhesion**

The mucoadhesive behaviour of the prepared CBPM was evaluated on sheep nasal mucosa using a method previously described by Belgamwar *et al.* [13]. Briefly, freshly cut sheep nasal mucosa was obtained from a local abattoir, cleaned, and rinsed with Simulated Nasal Electrolyte Solution (SNES). A 5 cm long strip of this tissue was mounted on a polyethylene plate and placed at an angle of 45°. Accurately weighed CBPM formulation (containing ~50 mg PGB) was carefully sprinkled on the tissue. Phosphate buffer (pH 6.6, pre-heated at 37 °C) was peristaltically pumped over the mucosa at a 5 ml/min rate for one hour. After one hour, the mucosal perfusate containing non-adhered microspheres was collected, diluted suitably, and the absorbance of the resulting solution was analyzed spectroscopically (Model: SPECTRO 2060 Plus, UV Spectra TM, Analytical Technologies Ltd., Gujarat, India) at 403 nm. The mucoadhesive potential was calculated according to the formula provided by Pardeshi *et al.* (30) and was expressed as percent mucoadhesion.

$$\textit{In vitro}\ \text{mucoadhesion}\ (\%) = \frac{\text{Amount of adhered microspheres}}{\text{Amount of applied microspheres}} \times 100$$

***In vitro* drug diffusion**

The diffusion efficiency of PGB from the design-optimized CBPM was studied using a glass-fabricated Franz diffusion cell, following the method described by Pardeshi *et al.* [28]. A dialysis membrane (LA395, Dialysis membrane-110, Average flat width ~ 31.71 mm, Average diameter~ 21.5 mm, Capacity ~ 3.63 ml/cm, and Pore size ~ 2.4 nm; HiMedia Laboratories, Mumbai, India) was used as a diffusion barrier. Before the study, the impurities were removed by rinsing the membrane as per the instructions provided by the manufacturer. After this, a sample of pure PGB (10 mg) or the prepared CBPM (containing ~10 mg of PGB) was dispensed onto the membrane between the donor and the receptor compartment. The phosphate buffer (pH 6.6, 12 ml) was used as a diffusion medium in the receptor compartment. The temperature of the dissolution medium was maintained at 37±1 °C using a water bath. At predetermined time intervals, samples (1 ml) were withdrawn, diluted suitably, and the absorbance of the resulting solution was analyzed using a UV-visible spectrophotometer (Model: SPECTRO 2060 Plus, UV Spectra TM, Analytical Technologies Ltd. Gujarat, India) at 403 nm to estimate the diffusion of PGB across the membrane.

***Ex-vivo* drug permeation studies**

The permeation efficiency of PGB from the prepared CBPM formulation across biological membranes was studied using a method previously reported by Tas *et al.* [29]. Briefly, freshly cut sheep nasal mucosa was obtained from a local abattoir, cleaned, and rinsed with Simulated Nasal Electrolyte Solution (SNES). After rinsing, the membrane was placed onto the Franz diffusion cell apparatus with a mucosal surface towards the donor compartment and a serosal surface towards the receptor compartment. The receptor compartment was filled with phosphate buffer (pH 6.6, 12 ml) maintained at 37 °C, with continuous stirring. The prepared CBPM formulation (containing ~10 mg of PGB) was loaded onto the mucosal surface of the mucosal tissue (donor compartment). As per predetermined time intervals, sample aliquots were retrieved, diluted appropriately, and analyzed for absorbance on a UV-visible spectrophotometer (Model: SPECTRO 2060 Plus, UV Spectra TM, Analytical Technologies Ltd. Gujarat, India) at 403 nm.

***In vivo* anticonvulsant activity**

The anticonvulsant activity of the prepared CBPM formulation was studied using a Pentylenetetrazol (PTZ)–induced seizure in the Albino mice model [30, 31].

Animals

Adult male Swiss Albino mice (Sprague Dawley®Strain, bred in-house, 22-25 g) University Department of Pharmaceutical Sciences, RTM Nagpur University, Nagpur, India, were used to evaluate the influence of pure PGB or optimized CBPM as an anticonvulsant on Pentylenetetrazol (PTZ)–induced seizure model. The animals were grouped and separately housed in colony cages maintained at a controlled temperature (25±5 °C) and humidity (50±5 % RH) conditions, with 12 h of light/dark cycle. The food (Pellet chow, Brook Bond, Lipton, India) and water were provided *ad libitum*. The experimental animal protocol (UDPS/IAEC/2016-17, dated 08/09/2016) was approved for this study by the Institutional Animal Ethical Committee (IAEC) of the University Department of Pharmaceutical Sciences, RTM Nagpur University, Nagpur, India. The approved protocol was followed according to the ethical guidelines provided by the Committee for the Purpose of Control and Supervision of Experiments on Animals.

Dosing

The experimental animals were divided into four groups of six animals each. The group I animals received the saline solution (0.9% w/v) and served as blank (negative control). Group II animals received the PTZ (80 mg/kg, sc) after 30 min of the saline solution and served as a positive control. Group III animals were anesthetized using light ketamine. A suspension of CBPM (dose: 4 mg/kg) in normal saline (0.9 % w/v) was administered intranasally *via* a polyethylene tube attached to a Hamilton syringe. Group IV animals received a suspension of CBPM (dose: 4 mg/kg) in normal saline (0.9 % w/v) *via the* intra-peritoneal route. Following 30 min of administering the formulations, groups III and IV received a single dose of PTZ (80 mg/kg, sc). The antiepileptic activity of CBPM in PTZ-induced seizures was assessed by recording the onset of clonic convulsions and percentage protection.

RESULTS AND DISCUSSION

Preparation of CBPM

The design-optimized CBPM was prepared using an ionotropic gelation method. Chitosan is a biocompatible, amphiphilic, poly-cationic polymer that shows reasonable solubility in water and other

organic solvents [32]. Previous literature reported deionized water (DI) as the solvent for solubilization and preparation of chitosan-based microsphere formulations [33]. Other studies reported the distilled water (DW) solvent for the preparation of microsphere formulations [34]. However, our preliminary solubility studies revealed poor solubility of chitosan in DI or DW, resulting in precipitation of chitosan from DI and DW during formulation. Thus, for effective solubilization of chitosan, other organic solvents were explored. We observed that dilute acetic acid (1 % v/v, pH<6) was an effective solvent for the solubilization of chitosan. The low pH of acetic acid may protonate the primary amino group of chitosan, resulting in the effective solubilization of chitosan [32]. Therefore, we primarily used dilute acetic acid (1 % v/v) as our solvent of choice in the preparation of CBPM.

Box-behnken design

The results of PGB inclusion efficiency obtained from the design-specified trial formulations are shown in table 2. The results indicated that all three selected variables had varying degrees of influence on the inclusion efficiency of PG Bin the prepared CBPM. The prepared trial formulations of CBPM exhibited PGB inclusion efficiencies of 50 to 96%. Upon analyzing the obtained results, the design of the experiments showed a quadratic model and the polynomial equation (below). From the equation, the conclusions were drawn based on the magnitude of the coefficients and the sign (+or-) associated with them.

$$Y = 85.42+4.07X_1+16.60\ X_2+2.82\ X_3-5.60X_1^2-5.94X_2^2-7.64X_3^2+1.22X_1X_2+4.51X_1X_3+3.98X_2X_3$$

Table 2: Box-behnken design experimental trial batches, with obtained yield values (%, w/w)

Experimental trials	X_1	X_2	X_3	Inclusion efficiency* (%, w/w)
1	0	+1	+1	93.37±1.17
2	-1	0	-1	68.19±1.54
3	0	0	0	78.73±0.67
4	+1	0	+1	85.20±1.78
5	+1	+1	0	96.04±1.20
6	+1	0	-1	65.11±1.56
7	-1	-1	0	54.17±0.87
8	-1	+1	0	83.24±0.78
9	+1	-1	0	62.08±1.12
10	0	-1	+1	50.52±1.54
11	-1	0	+1	70.23±0.34
12	0	+1	-1	85.20±1.67
13	0	-1	-1	58.27±1.87
14	0	0	0	89.76±1.90
15	0	0	0	76.92±1.61
16	0	0	0	91.21±1.76
17	0	0	0	90.47±1.85

*Values are represented mean±Std. Dev. (n = 3)

Among the different values obtained for the magnitude of coefficients from the equation, the value of b_2, and b_3 were found to be statistically significant (p<0.05); whereas those for b_0, b_1, b_3, b_{11}, b_{22}, b_{33}, b_{12}, b_{13}, and b_{23} were insignificant. The calculated F value (9.07) was also statistically significant. Moreover, the positive (+) sign associated with the coefficients b_1, b_2, and b_3 indicated a direct correlation between the study variables and the PGB inclusion efficiency. These observations concluded that the developed model best represents the influence of studied variables on the inclusion efficiency of PGB in the prepared CBPM. The response surface and contour plots (fig. 1) further explain the studied variables' influence on the PGB inclusion efficiency. Additionally, a numerical optimization process was applied to optimize the variables. Based on this process, trial formulation #16 displayed the optimal values of the studied variables. These values were 150 mg, 1000 RPM, and 1.5 ml for the amount of chitosan, stirring speed, and cross-linking agent, respectively.

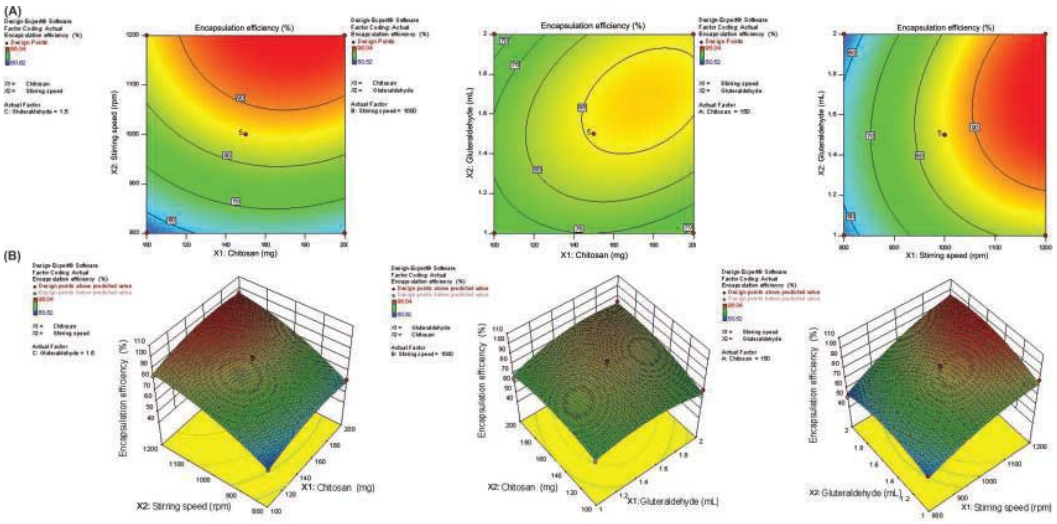

Fig. 1: a) Counter plot and b) response surface plot of inclusion efficiency (%, Y) as a function of the amount of chitosan (X_1, mg), stirring speed (X_2, RPM), and cross-linking agent (X_3, ml)

Validation of the optimized model

An additional formulation of CBPM was prepared using the optimal values of the variables obtained from the model to validate the developed model. The PGB inclusion efficiency obtained from this formulation was then compared with the model-predicted (theoretical) value. The results showed that the PGB inclusion efficiency obtained from this additional formulation (91.45 % w/w) was slightly higher than the model-predicted value (89.41 % w/w). The relative robustness of the model was also confirmed by the lower bias value (-2.28 %) calculated using the equation below.

$$\text{Bias (\%)} = \frac{\text{Predicted value} - \text{observed value}}{\text{Predicted value}} \times 100$$

Particle size and zetapotential

Particle size, size distribution, and zeta potential are essential properties of multiparticulate systems, indicating their physical stability, distribution, and bioavailability upon administration. An earlier report by Pardeshi *et al.* suggested that prepared microspheres with particle sizes of 10 to 22 µm favour mucoadhesion and intranasal delivery [28]. The particle size ad zeta potential of CBPM formulations are discussed below. The mean particle size of the prepared CBPM was 18.40±0.33 µm, suggesting its suitability for intranasal administration. The polydispersity index was found to be 0.36±0.03, indicating a narrow particle size distribution. Zeta potential (ζ) is a valuable tool for determining surface charges and a potential indicator of the physical stability of microscopic multiparticulate systems. Zeta potential measures the magnitude of charges on the particles. Higher values (positive or negative) indicate the strength of a multiparticulate dispersion. Typically, a value of >30 mV indicates good stability [35]. The zeta potential value of this formulation was 32.0±0.25 mV, indicating excellent stability. Thus, the particle size analysis and zeta potential estimation results ascertained nasal administration's physical stability and suitability.

SEM analysis

(fig. 2a and 2b) shows a comparison of the surface morphologies of pure PGB and the design-optimized CBPM as observed by scanning electron microscopy. The micrographs of pure PGB exhibited highly ordered crystalline particles. The particles of pure PGB appeared to be varying sizes of laminar crystals. As expected, the particles of CBPM formulations were dramatically different from those of pure PGB. True to their definition, the microsphere was observed to have a spherical particle shape with a relatively smooth surface. The micrographs of CBPM did not reveal any signs of rupture, cracks, or pores. Previous reports have suggested microspheres with a spherical and smooth surface can slow nasal clearance, increase nasal deposition, and increase bioavailability [36].

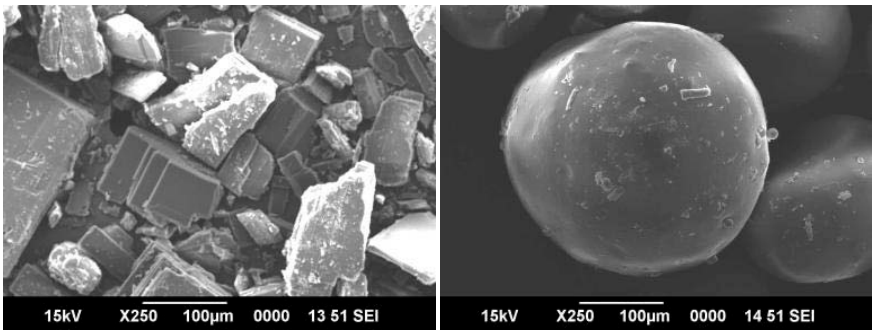

a) **b)**

Fig. 2: SEM images of a) pure PGB and b) design-optimized CBPM formulations

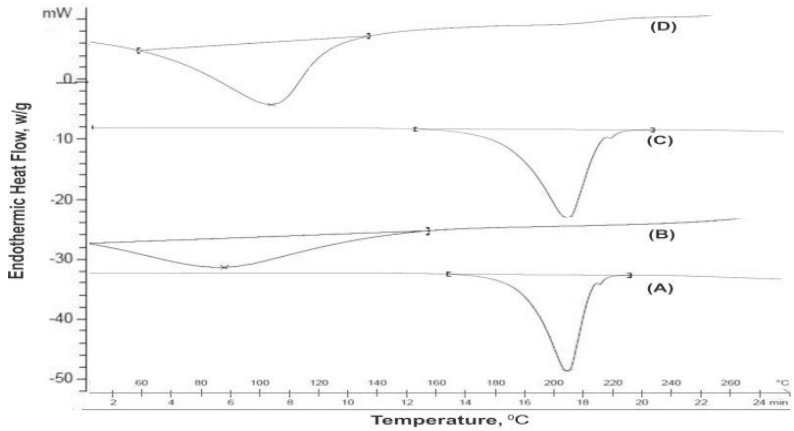

Fig. 3: DSC thermograms of a) Pure PGB, b) Pure chitosan, c) PM, d) design-optimized CBPM formulations

Thermal analysis

Thermal analysis of pharmaceutical materials is a valuable tool in determining the stability and compatibilities between formulation components. Fig. 3 (a, b, c, and d) shows the DSC thermograms of pure PGB, pure chitosan, PM, and CBPM. The thermogram of pure PGB (fig. 3a) exhibited a single, sharp, endothermic melting peak around 200 °C. This peak indicated the purity and crystalline nature of PGB and was consistent with earlier findings [2]. The thermogram of pure chitosan (fig. 3b) showed a single, broad, and diffused endothermic peak with low intensity, around 85 °C, indicating the melting temperature range of chitosan [14, 36]. The thermogram of PM (fig. 3c) exhibited a relatively broader endothermic peak corresponding to that of pure PGB. The lack of chitosan characteristics in the peak can be attributed to the lower quantity of chitosan in the mixture. Finally, the thermogram of CBPM (fig. 3d) showed a new broad endothermic peak around 89 °C, with the disappearance of individual peaks of pure PGB and chitosan. The

formation of a broad peak of CBPM and the disappearance of peak after PGB. The peak can be attributed to decreasing the crystallinity and partial amorphization of pure PGB [14, 36]. Thus, from comparing the above thermograms, it can be suggested that stable microspheres of chitosan and PGB were formed by weak intermolecular interactions (hydrogen bonding, van der Waals interactions) between chitosan and PCB.

FT-IR

The spectra obtained from the FT-IR analysis of pure PGB, pure chitosan, PM, and CBPM are shown in fig. 4 (a, b, c, and d), respectively. The spectrum of pure PGB (fig. 4a) showed important characteristic absorption peaks at 2956.48 cm-1 (N-H stretching), 2600.98 cm-1(O-H stretching) and 1645.23 cm-1 (C=O stretching). These observed peaks are consistent with those reported earlier [1]. The spectrum of chitosan (fig. 4b) exhibited absorption peaks at 3443.32 cm-1(O-H stretching), 2880.38 cm-1(C-H stretching), and 1654.60 cm-1(N-H stretching). Additional peaks were observed at 1378.72 cm-1 (amide group) and 1091.45 cm-1 (C=O stretching in the C-O-C group). These observations were also consistent with previously reported results [37]. The FTIR spectrum of PM (fig. 4c) displayed characteristic peaks of pure PGB and chitosan. These peaks were observed at 3442.18 cm-1, 2955.00 cm-1, 2601.60 cm-1, 1644.82 cm-1, 1391.98 cm-1and 1100.01 cm-1. The spectrum of CBPM (fig. 4d) showed characteristic absorption peaks at 3436.90 cm-1(O-H stretching), 2940.80 cm-1(N-H stretching), 1642.23 cm-1(C=O stretching), 1399.82 cm-1(amide group) and 1115.33 cm-1(C=O stretching in C-O-C group). The appearance, disappearance, and shifting of new peaks in CBPM could be attributed to the interaction between pure PGB and chitosan. With these interactions, the characteristic absorption peaks associated with pure PGB, i.e., at 2956.48 cm-1 and 1645.25 cm-1 were shifted to 2940.80 cm-1 and 1642.23 cm-1, respectively. Specific peaks associated with chitosan, i.e., at 3443.32 cm-1, 2880.38 cm-1and 1654.60 cm-1appeared to shift to 3442.18 cm-1, 2955.00 cm-1, and 1644.82 cm-1, respectively. Therefore, the appearance and shifting of characteristic peaks can be attributed to weak intermolecular interaction leading to the formation of the stable CBPM microsphere. It can thus be surmised that the formation of CBPM involved weak intermolecular interactions between PGB and chitosan.

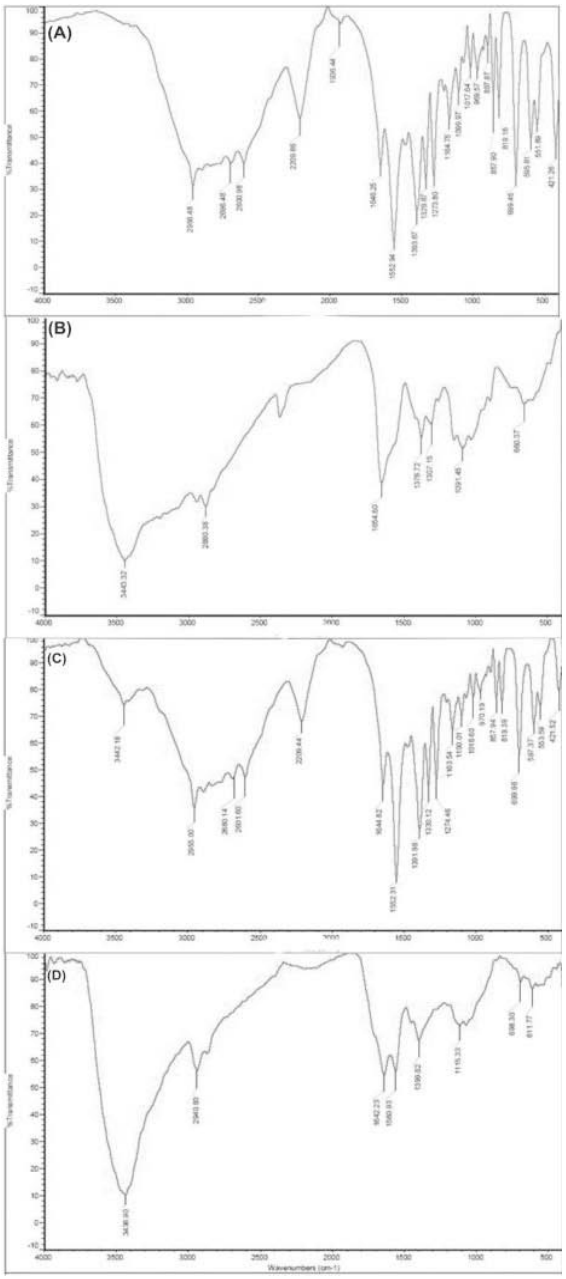

Fig. 4: FTIR spectrum of a) Pure PGB b) Pure chitosan c) PM d) Design-optimized CBPM formulation

PXRD

Fig. 5 (a, b, c, and d) displays the x-ray diffractograms of pure PGB, chitosan, PM, and the prepared CBPM. The diffraction pattern of pure PGB (fig. 5a) showed characteristic, sharp, intense peaks at 10°, 17°, 19°, 22°, 24°, 27°, 30°, 36°, 39°, and 41° 2θ, indicating the highly crystalline nature of PGB. These patterns were consistent with those reported earlier [38]. (fig. 5b) shows the diffraction pattern of pure chitosan. The diffractograms exhibited two different characteristic peaks. Both peaks were relatively broad and appeared at 10° and 20° with high intensity. These peaks can be attributed to the crystallinity of chitosan and the hydrogen bonding between the amino groups of the chitosan molecule. Similar observations concerning an x-ray diffraction pattern of chitosan were reported earlier [39]. The diffraction pattern of PM (fig. 5c) showed characteristic peaks associated with pure PGB and chitosan. A small number of crystalline peaks with lower intensity were associated with PGB and can be assumed to be due to a lower amount of PGB present in the PM. In contrast, the prominent and broader peaks with higher intensity may be related to chitosan. Finally, the diffraction pattern of optimized CBPM (fig. 5d) exhibited a complete absence of crystalline peaks of PGB. The lack of crystalline peaks might be attributed to the dispersion of PGB into the chitosan polymer matrix at a molecular level and the partial amorphization of PGB. These results are supported by the previously reported observations [13, 14, 40].

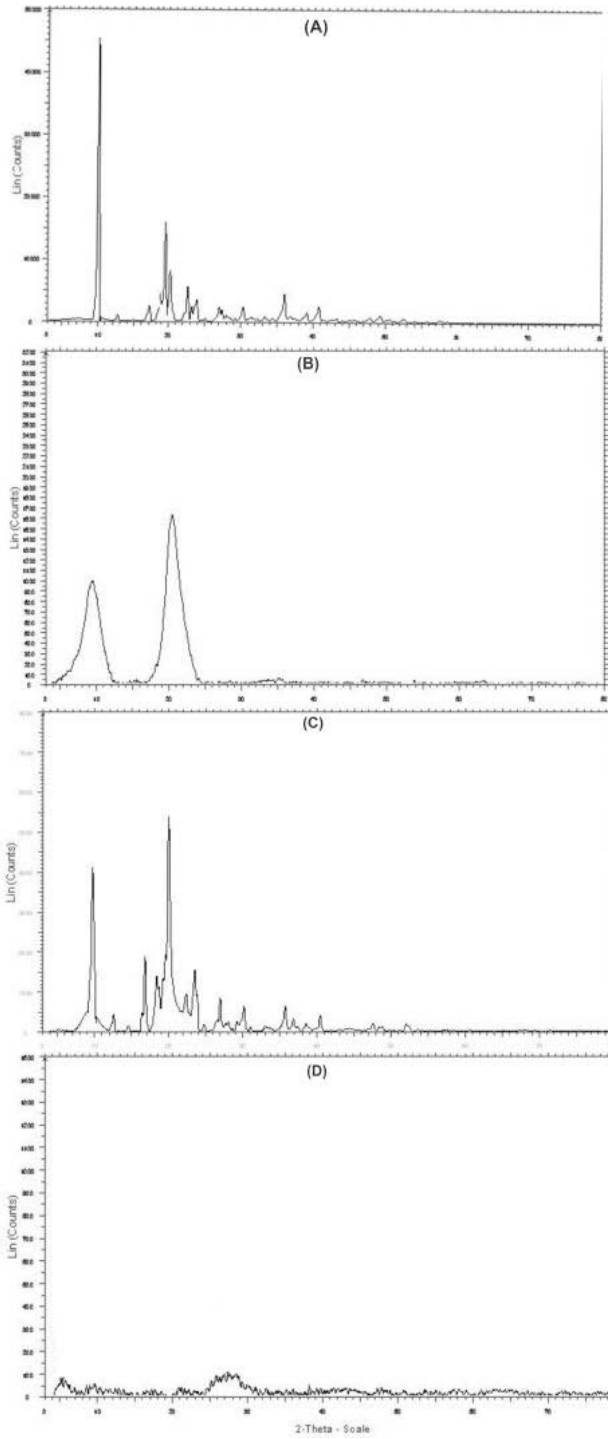

Fig. 5: PXRD spectrum of a) Pure PGB b) Pure chitosan c) PM d)Design-optimized CBPM formulations

In vitro mucoadhesion

The mucoadhesive potential of the prepared CBPM was 80.21±1.19 % (n=3), indicating excellent adhesivity of the prepared microsphere formulation on the sheep nasal mucosa. The mucoadhesive properties of chitosan are widely reported [41]. The presence of positively charged amino groups in chitosan polymer demonstrates electrostatic interactions with negatively charged sialic and sulfonic acid groups in the nasal mucosa, resulting in effective mucoadhesion. Moreover, when cross-linked with optimal amounts of glutaraldehyde, chitosan improves the flexibility of chitosan, resulting in the formation of microspheres that possess liquid-gel characteristics and high aqueous solubility, and easy penetrability into the mucus epithelial layers. These combined influences greatly facilitate mucoadhesion. The results obtained to follow the previously published reports [39].

In vitro diffusion

Fig. 6 shows the *in vitro* diffusion profile of PGB from the prepared CBPM formulation across a dialysis membrane. As shown in fig. 6, the rate and extent of diffusion of pure PGB across the dialysis membrane were significantly lower than that of the prepared CBPM. At the end of 90 min, only about ~70 % of pure PGB permeated across the membrane. Conversely, the CBPM exhibited an increased and steady diffusion of PGB across the membrane. At the end of the testing period, over 90 % of PGB was found to have diffused across the membrane. The observed initial burst release (0-10 min) of PGB could be due to the excess amount of PGB on the surface of the microspheres. These observations are consistent with the findings earlier [13, 28]. The kinetics and the mechanism of PGB release from the optimized CBPM were assessed using several kinetic models, viz. zero order, first order, Higuchi, and Korsmeyer-Peppas models. The release kinetics appeared to fit all models with varying degrees. However, upon closer inspection of the regression coefficient (*R2*), zero-order was observed to be the best fit (*R2* = 0.9908) kinetic model describing the diffusion and release kinetics of PGB from CBPM. The release exponent value (n = 0.63) indicated a non-Fickian or anomalous diffusion mechanism.

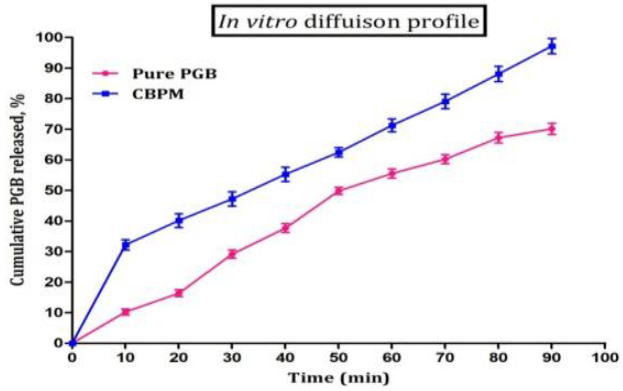

Fig. 6: The *in vitro* diffusion profile of pure PGB and design-optimized CBPM formulations across the dialysis membrane, Values are mean±Std. Dev (n = 3)

Ex vivo permeation

The comparative *ex vivo* permeation behaviour of pure PGB and PGB from CBPM across the sheep nasal mucosa is shown in (fig. 7). Similar to the *in vitro* diffusion results, the rate and extent of permeation of pure PGB across the sheep nasal mucosa were significantly lower than that of the prepared CBPM. At the end of the permeation study period, only about ~77% of pure PGB were able to cross the biological membrane. Conversely, the CBPM demonstrated an increased and steady permeation of PGB across the mucosa. At the end of the testing period, over 90 % of PGB was found to have permeated across the mucosal membrane. The *ex vivo* permeability profiles of pure PGB and PGB from CBPM closely match their respective *in vitro* diffusion profiles.

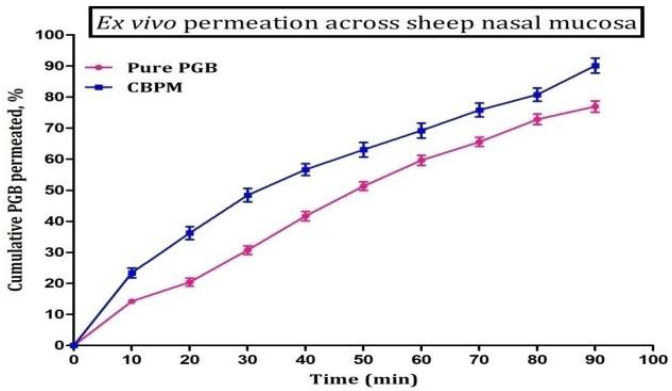

Fig. 7: The *ex vivo* permeation profile of pure PGB and design-optimized CBPM formulations across sheep nasal mucosa, values are mean±Std. Dev (n = 3)

In vivo anticonvulsant activity

Fig. 8 shows the comparative results of the anticonvulsant activity of CBPM in PTZ-induced seizures in a Swiss albino mice model, administered either *via* the intraperitoneal route or *via* the intranasal route. The animals that received PTZ alone showed an earlier and severe ($p<0.05$) onset of clonic seizures and resulted in 100% mortality, i.e., all animals receiving PTZ alone died within a

few minutes. The animals receiving CBPM (4 mg/kg) by intra-peritoneal route significantly ($p<0.05$) delayed the onset of clonic convulsions and demonstrated up to 33.33% protection against PTZ-induced mortality. Finally, the animals receiving CBPM (4 mg/kg) also delayed the onset of convulsions significantly ($p<0.01$) and exhibited significantly higher (66.66%) protection against PTZ-induced mortality. The overall results demonstrate the improved therapeutic effectiveness of CBPM *via* intranasal administration.

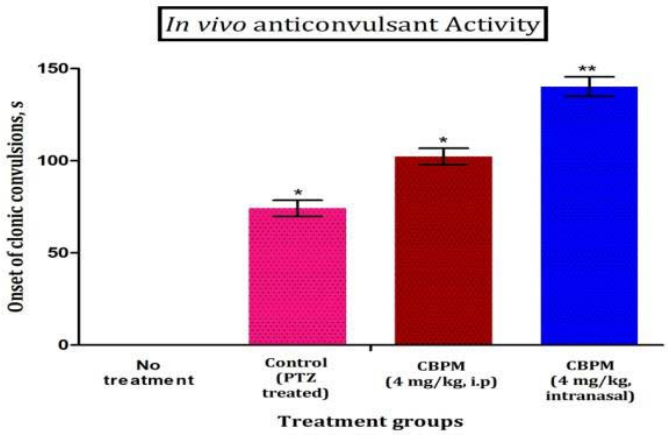

Fig. 8: Influence of design-optimized CBPM formulations at a dose of (4 mg/kg) via the intra-peritoneal or intranasal route in PTZ-induced seizures in the swiss albino mice model

CONCLUSION

The presented study prepared a chitosan-based, mucoadhesive, microsphere formulation of PGB using a relatively simple, reproducible, inotropic-gelation method. The formulation and process variables were optimized using the Box-behnken design. The physico-chemical characterization of the prepared formulation supported the formation of microspheres and indicated the involvement of weak intermolecular interactions between PGB and chitosan. The ready CBPM formulation exhibited acceptable mucoadhesive properties attributable to the electrostatic interactions between chitosan and mucosal components. The *in vitro* diffusion and the *ex vivo* permeation studies showed increased permeability of PGB from the prepared CBPM across the dialysis and biological membrane, respectively. The preliminary pharmacological evaluation exhibited a significant therapeutic benefit offered by CBPM to delay PTZ-induced clonic convulsions and protect against PTZ-induced mortality in mice. The study provides the feasibility of developing an intranasal microsphere formulation as an alternative approach for the delivery of PGB. Further studies are warranted better to understand the system's formulation and other functional aspects.

ACKNOWLEDGEMENT

The authors and corresponding authors express their gratitude to the management of Datta Meghe College of Pharmacy, DMIMS (DU), for providing research facilities and financial and technical support to complete this manuscript on time.

FUNDING

Nil

AUTHORS CONTRIBUTIONS

All the authors have contributed equally.

CONFLICT OF INTERESTS

The authors declare no conflict of interest

REFERENCES

1. Kanwar N, Kumar R, Sarwal A, Sinha VR. Preparation and evaluation of floating tablets of pregabalin. Drug Dev Ind Pharm. 2016;42(4):654-60. doi: 10.3109/03639045.2015.1062895. PMID 26146770.
2. Aydogan E, Comoglu T, Pehlivanoglu B, Dogan M, Comoglu S, Dogan A. Process and formulation variables of pregabalin microspheres prepared by w/o/o double emulsion solvent diffusion method and their clinical application by animal modeling studies. Drug Dev Ind Pharm. 2015;41(8):1311-20. doi: 10.3109/03639045.2014.948452. PMID 25119000.
3. Gujral RS, Haque SM, Kumar SA. A novel method for the determination of pregabalin in bulk pharmaceutical formulations and human urine samples. Afr J Pharm Pharmacol. 2009 Jun;3(6):327-34.
4. Ben Manachem E. Pregabalin pharmacology ad its relevance to clinical practice. Epilepsia. 2004 Aug;45(6):13-8. doi: 10.1111/j02213-9580.2004.455003.x.
5. Bockbrader HN, Radulovic LL, Posvar EL, Strand JC, Alvey CW, Busch JA. Clinical pharmacokinetics of pregabalin in healthy volunteers. J Clin Pharmacol. 2010;50(8):941-50. doi: 10.1177/0091270009352087, PMID 20147618.
6. Finnerup N. Clinical use of pregabalin in the management of central neuropathic pain. Neuropsychiatr Dis Treat. 2007;Dec 3:3(6):885-91. doi: 10.2147/NDT.S1715.
7. Arafa MG, Ayoub BM. DOE optimization of nano-based carrier of pregabalin as hydrogel: new therapeutic & chemometric approaches for controlled drug delivery systems. Sci Rep. 2017 Jan 30;7(1):1-15. doi: 10.1038/srep41503.
8. Fukasawa H, Muratake H, Nagae M, Sugiyama K, Shudo K. Transdermal administration of aqueous pregabalin solution as a potential treatment option for patients with neuropathic pain to avoid central nervous system-mediated side effects. Biol Pharm Bull. 2014;37(11):1816-9. doi: 10.1248/bpb.b14-00278. PMID 25212662.
9. Jeong KH, Woo HS, Kim CJ, Lee KH, Jeon JY, Lee SY. Formulation of a modified-release pregabalin tablet using hot-melt coating with glyceryl behenate. Int J Pharm. 2015;495(1):1-8. doi: 10.1016/j.ijpharm.2015.08.057. PMID 26315121.
10. Acikgoz M, Kas HS, Orman M, Hincal AA. Chitosan microspheres of diclofenac sodium: I. Application of factorial design and evaluation of release kinetics. J Microencapsul. 1996;13(2):141-59. doi: 10.3109/02652049609052903, PMID 8999120.
11. Agnihotri SA, Aminabhavi TM. Controlled release of clozapine through chitosan microparticles prepared by a novel method. J Control Release. 2004;96(2):245-59. doi: 10.1016/j.jconrel.2004.01.025, PMID 15081216.
12. Martinac A, Filipovic Grcic J, Voinovich D, Perissutti B, Franceschinis E. Development and bioadhesive properties of chitosan-ethylcellulose microspheres for nasal delivery. Int J Pharm. 2005;291(1-2):69-77. doi: 10.1016/j.ijpharm.2004.07.044. PMID 15707733.

13. Belgamwar VS, Patel HS, Joshi AS, Agrawal A, Surana SJ, Tekade AR. Design and development of nasal mucoadhesive microspheres containing tramadol HCl for CNS targeting. Drug Deliv. 2011;18(5):353-60. doi: 10.3109/10717544.2011.557787, PMID 21351825.
14. Patel D, Singh S. Chitosan: a multifacet polymer. Int J Curr Pharm. 2015;7(2):21-8.
15. Nayak UY, Gopal S, Mutalik S, Ranjith AK, Reddy MS, Gupta P. Glutaraldehyde cross-linked chitosan microspheres for controlled delivery of zidovudine. J Microencapsul. 2009 Apr 14;26(3):214-22. doi: 10.1080/02652040802246325, PMID 18819029.
16. Thanoo BC, Sunny MC, Jayakrishnan A. Cross-linked chitosan microspheres: preparation and evaluation as a matrix for the controlled release of pharmaceuticals. J Pharm Pharmacol. 1992;44(4):283-6. doi: 10.1111/j.2042-7158.1992.tb03607.x. PMID 1355537.
17. Dhanaraju MD, Elizabeth S, Gunasekaran T. Triamcinolone-loaded glutaraldehyde cross-linked chitosan microspheres: prolonged-release approach for the treatment of rheumatoid arthritis. Drug Deliv. 2011;18(3):198-207. doi: 10.3109/10717544.2010.528069, PMID 21028952.
18. Agrawal M, Saraf S, Saraf S, Antimisiaris SG, Chougule MB, Shoyele SA. Nose-to-brain drug delivery: an update on clinical challenges and progress towards approval of anti-Alzheimer drugs. J Control Release. 2018;281:139-77. doi: 10.1016/j.jconrel.2018.05.011. PMID 29772289.
19. Crowe TP, Greenlee MHW, Kanthasamy AG, Hsu WH. Mechanism of intranasal drug delivery directly to the brain. Life Sci. 2018;195:44-52. doi: 10.1016/j.lfs.2017.12.025. PMID 29277310.
20. Laffleur F, Bauer B. Progress in nasal drug delivery systems. Int J Pharm. 2021 Aug 12;607:120994. doi: 10.1016/j.ijpharm.2021.120994. PMID 34390810.
21. Pani NR, Acharya S, Patra S. Development and validation of RP-HPLC method for quantification of glipizide in biological macromolecules. Int J Biol Macromol. 2014 Jan 10;65:65-71. doi: 10.1016/j.ijbiomac.2014.01.007. PMID 24418334.
22. Jeffery H, Davis SS, O'Hagan DT. The preparation and characterization of poly(lactide-co-glycolide) microparticles. I: Oil-in-water emulsion solvent evaporation. International Journal of Pharmaceutics. 1991;77(2-3):169-75. doi: 10.1016/0378-5173(91)90314-E.
23. Ararath D, Velmurugan S. Formulation and evaluation of nevirapine mucoadhesive microspheres. Int J Pharm Pharm Sci. 2015;7(6):342-8.
24. Sahu VK, Sharma N, Sahu PK, Saraf SA. Formulation and evaluation of floating-mucoadhesive microspheres of novel natural polysaccharide for site specific delivery of ranitidine hydrochloride. Int J App Pharm. 2017;9(3):15-9. doi: 10.22159/ijap.2017v9i3.16137.
25. Velmurugan S, Ashraf MA. Preparation and evaluation of maraviroc mucoadhesive microspheres for gastro retentive drug delivery. Int J Pharm Pharm Sci. 2015;7(5):208-14.
26. Deshmukh MT, Mohite SK. Formulation and characterization of olanzepineloaded mucoadhesive microspheres. Asian J Pharm Clin Res 2017;10(4):16659. doi: 10.22159/ajpcr.2017.v10i4.16659.
27. Lal K, Purohit A, Ram H. Glucose homeostatic and pancreas protective potential of tecomella undulata root extract in streptozotocin induced diabetic rats. Asian J Pharm Clin Res. 2017;10(6):17997. doi: 10.22159/ajpcr.2017.v10i6.17997.
28. Pardeshi CV, Rajput PV, Belgamwar VS, Tekade AR. Formulation, optimization and evaluation of spray-dried mucoadhesive microspheres as intranasal carriers for valsartan. J Microencapsul. 2012;29(2):103-14. doi: 10.3109/02652048.2011.630106, PMID 22047546.
29. Tas C, Ozkan C, Savaser A, Ozkan Y, Tasdemir U, Altunay H. Nasal absorption of metoclopramide from different Carbopol® 981 based formulations: *in vitro*, *ex vivo* and *in vivo* evaluation☆. European Journal of Pharmaceutics and Biopharmaceutics. 2006;64(2):246-54. doi: 10.1016/j.ejpb.2006.05.017.
30. Kasture VS, Kasture SB, Chopde CT. Anticonvulsive activity of Butea monosperma flowers in laboratory animals. Pharmacol Biochem Behav. 2002;72(4):965-72. doi: 10.1016/S0091-3057(02)00815-8, PMID 12062587.
31. Serralheiro A, Alves G, Fortuna A, Falcao A. Direct nose-to-brain delivery of lamotrigine following intranasal administration to mice. Int J Pharm. 2015;490(1-2):39-46. doi: 10.1016/j.ijpharm.2015.05.021, PMID 25979854.
32. Pillai CKS, Paul W, Sharma CP. Chitin and chitosan polymers: Chemistry, solubility and fiber formation. Prog Polym Sci. 2009;34(7):641-78. doi: 10.1016/j.progpolymsci.2009.04.001.
33. Aramwit P, Ekasit S, Yamdech R. The development of non-toxic ionic-crosslinked chitosan-based microspheres as carriers for the controlled release of silk sericin. Biomed Microdevices. 2015 Aug 2;17(5):84. doi: 10.1007/s10544-015-9991-4, PMID 26233725.
34. Pandey R, Khuller GK. Chemotherapeutic potential of alginate-chitosan microspheres as anti-tubercular drug carriers. J Antimicrob Chemother. 2004;53(4):635-40. doi: 10.1093/jac/dkh139, PMID 14998985.
35. Freitas C, Muller RH. Effect of light and temperature on zeta potential and physical stability in solid lipid nanoparticle (SLN™) dispersions. International Journal of Pharmaceutics. 1998;168(2):221-9. doi: 10.1016/S0378-5173(98)00092-1.
36. Kulkarni AD, Bari DB, Surana SJ, Pardeshi CV. *In vitro*, ex vivo and *in vivo* performance of chitosan-based spray-dried nasal mucoadhesive microspheres of diltiazem hydrochloride. J Drug Deliv Sci Technol. 2016;31:108-17. doi: 10.1016/j.jddst.2015.12.004.
37. Mohammed MH, Williams PA, Tverezovskaya O. Extraction of chitin from prawn shells and conversion to low molecular mass chitosan. Food Hydrocoll. 2013;31(2):166-71. doi: 10.1016/j.foodhyd.2012.10.021.
38. Bhaskarbhai J, Chandra Has Khanduri SBJ. Polymorphic form I of pregabalin and process for its preparation. United States Pat Appl. 2006;1:1-8.
39. Pardeshi CV, Belgamwar VS. Controlled synthesis of N,N,N-trimethyl chitosan for modulated bioadhesion and nasal membrane permeability. Int J Biol Macromol. 2016;82:933-44. doi: 10.1016/j.ijbiomac.2015.11.012, PMID 26562548.
40. Jain SA, Chauk DS, Mahajan HS, Tekade AR, Gattani SG. Formulation and evaluation of nasal mucoadhesive microspheres of sumatriptan succinate. J Microencapsul. 2009;26(8):711-21. doi: 10.3109/02652040802685241, PMID 19888880.
41. Dash M, Chiellini F, Ottenbrite RM, Chiellini E. Chitosan-a versatile semi-synthetic polymer in biomedical applications. Prog Polym Sci. 2011;36(8):981-1014. doi: 10.1016/j.progpolymsci.2011.02.001.
42. Sahu VK, Sharma N, Sahu PK, Saraf SA. Formulation and evaluation of floating-mucoadhesive microspheres of novel natural polysaccharide for site specific delivery of ranitidine hydrochloride. Int J App Pharm. 2017;9(3):15-9. doi: 10.22159/ijap.2017v9i3.16137.